Use of Glancing Angle X-Ray Powder Diffractometry to Depth-Profile Phase Transformations During Dissolution of Indomethacin and Theophylline Tablets

Smita Debnath,[1] Paul Predecki,[2] and Raj Suryanarayanan[1,3]

Received July 8, 2003; accepted September 19, 2003

Purpose. The purpose of this study was (i) to develop glancing angle x-ray powder diffractometry (XRD) as a method for profiling phase transformations as a function of tablet depth; and (ii) to apply this technique to (a) study indomethacin crystallization during dissolution of partially amorphous indomethacin tablets and to (b) profile anhydrate → hydrate transformations during dissolution of theophylline tablets.

Methods. The intrinsic dissolution rates of indomethacin and theophylline were determined after different pharmaceutical processing steps. Phase transformations during dissolution were evaluated by various techniques. Transformation in the bulk and on the tablet surface was characterized by conventional XRD and scanning electron microscopy, respectively. Glancing angle XRD enabled us to profile these transformations as a function of depth from the tablet surface.

Results. Pharmaceutical processing resulted in a decrease in crystallinity of both indomethacin and theophylline. When placed in contact with the dissolution medium, while indomethacin recrystallized, theophylline anhydrate rapidly converted to theophylline monohydrate. Due to intimate contact with the dissolution medium, drug transformation occurred to a greater extent at or near the tablet surface. Glancing angle XRD enabled us to depth profile the extent of phase transformations as a function of the distance from the tablet surface. The processed sample (both indomethacin and theophylline) transformed more rapidly than did the corresponding unprocessed drug. Several challenges associated with the glancing angle technique, that is, the effects of sorbed water, phase transformations during the experimental timescale, and the influence of phase transformation on penetration depth, were addressed.

Conclusions. Increased solubility, and consequently dissolution rate, is one of the potential advantages of metastable phases. This advantage is negated if, during dissolution, the metastable to stable transformation rate ≫ dissolution rate. Glancing angle XRD enabled us to quantify and thereby profile phase transformations as a function of compact depth. The technique has potential utility in monitoring surface reactions, both chemical decomposition and physical transformations, in pharmaceutical systems.

KEY WORDS: amorphous; crystallization; dissolution; glancing angle; hydrate; x-ray powder diffractometry.

INTRODUCTION

Dissolution rate serves as an important quality control test that can provide information regarding batch-to-batch consistency of solid dosage forms (1). The monograph of every immediate-release tablet formulation in the *United States Pharmacopeia* stipulates the percentage of the labeled active pharmaceutical ingredient (API) that should dissolve in the specified time. The dissolution behavior of the API will be influenced by its physical form; that is, the polymorphic form, degree of crystallinity, and the state of solvation. Thermodynamically, the free energy difference between the metastable and stable forms of a compound dictates the difference in solubility and dissolution rate. While metastable phases can enhance dissolution rate, and in selected cases the bioavailability (2–4), their use in dosage forms is limited by physical and chemical stability issues.

Even when the stable form of an API is used for dosage form manufacture, phase transformation induced during processing can result in the inadvertent inclusion of a metastable form in the final product. It is being increasingly recognized by regulatory agencies that such processing-induced phase transitions can have a significant impact on the product performance, including dissolution. Therefore, the FDA provides guidance, in the form of decision trees, on when and how the solid state of drug should be controlled and monitored not only in the raw material, but also in the finished product (5). Numerous studies have reported the influence of both solid state of drug as well as processing conditions on drug dissolution rates (6–9).

Yet another factor that can influence drug dissolution rate is the metastable → stable transformation *during* dissolution. The amorphous forms of indomethacin (10), piretanide (6), and lactose (11) crystallize into their respective stable forms during dissolution. As a result, the calculated solubility and dissolution rate of metastable forms may not be actualized as is evident from several examples in the literature (10). Therefore, from a quality control as well as product performance perspective, it is important to characterize these transformations.

Because the surface is in intimate contact with the medium, the rate as well as extent of these transformations will be maximum at or near the surface of the dissolving particle. Hence, when dealing with tablet dissolution, there is a need to evaluate the extent of these conversions as a function of tablet depth. The influence of physical transformation on drug dissolution rates can be understood from such depth-profiling studies. However, the commonly used techniques for physical characterization including x-ray powder diffractometry (XRD), differential scanning calorimetry (DSC), infrared spectroscopy (IR), and scanning electron microscopy (SEM) were found to be unsuitable for the purpose. Although XRD is an excellent technique for the characterization of crystalline phases, the x-rays can penetrate up to a depth of several hundred micrometers and the information obtained is an average over this entire depth of penetration. SEM can at best provide qualitative information, and while both IR and Raman spectroscopy can be used for solid-phase quantification, they do not enable depth-profiling studies.

Glancing angle XRD, a technique wherein the x-rays are incident on the sample surface at a low angle (Fig. 1a), was deemed suitable to profile these transformations as a function of depth. This approach has previously been used to analyze the residual stress and strain as a function of depth at or near

[1] College of Pharmacy, University of Minnesota, Minneapolis, Minnesota 55455.

[2] Engineering Department, University of Denver, Denver, Colorado 80208.

[3] To whom correspondence should be addressed. (e-mail: surya001@umn.edu)

0724-8741/04/0100-0149/0

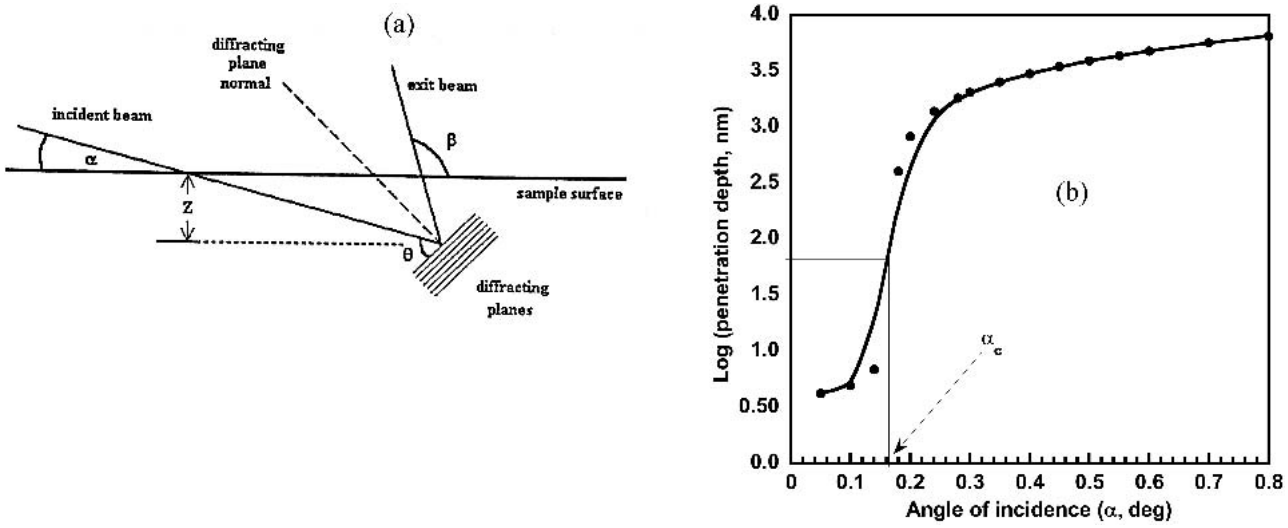

Fig. 1. Schematic representation of glancing angle x-ray diffractometry (33). Symbols are explained in the text. Reproduced with the permission of the copyright owner. (b) Representative theoretical plot of depth of penetration against angle of incidence for indomethacin. This plot was generated using Eq. (1). α_c is the critical angle of incidence.

the surface of thin semiconductor films (12), to determine change in composition with depth (13), and also for phase identification in multicomponent thin films (14). For example, a multilayer film of $CuIn_2Se_{3.5}/CuInSe_2/Mo$ was characterized and the thickness of the surface layer of $CuIn_2Se_{3.5}$ was determined to be ~9000 Å (13). However, to the best of our knowledge, the technique has not been used to study organic materials including pharmaceuticals.

In glancing angle XRD, the depth of x-ray penetration is a function of the angle of incidence (α, in radians) and can be determined by the Parratt equation (13,15,16),

$$\tau(\alpha) = \left(\frac{\lambda}{4\pi}\right)\left(\frac{\{[(\alpha^2-\alpha_c{}^2)^2+4\beta^2]^{1/2}+\alpha^2-\alpha_c{}^2\}}{2}\right)^{-1/2} \quad (1)$$

where τ is the irradiated depth of penetration (in meters), λ is the wavelength of x-rays (1.54 Å for Cu Kα radiation), $\beta = \mu\lambda/4\pi$ (μ is the mass attenuation coefficient), and the critical angle of incidence (in radians) is given by

$$\alpha_c = \cos^{-1}(1-\delta) \quad (2)$$

Total external reflection occurs at very low α, and α_c typically ranges from 0.2° to 0.6° (17). As α increases, the total external reflection decreases rapidly. This decrease is highest at the critical angle of incidence (α_c). In Eq. (2), δ, the real part of the complex refractive index, is defined as

$$\delta = \frac{Ne^2\lambda^2}{4\pi\varepsilon_0(2\pi mc^2)} \quad (3)$$

where $\varepsilon_0 = 8.85 \times 10^{-12}\ C^2N^{-1}m^{-2}$ (permittivity of vacuum), *e* and *m* are the charge and mass of the electron, respectively, *c* is the velocity of light, and *N* is the number of electrons per unit volume irradiated.

For a single-element specimen,

$$N = \frac{\rho N_{av} \times (Z + \Delta f')}{M} \quad (4)$$

where ρ is the density, N_{av} is the Avogadro number, *Z* is the atomic number, *M* is the atomic weight (kg/mole), and $\Delta f'$ is the real part of the dispersion correction to the scattering factor (18).

For a compound A_xB_y,

$$N = \frac{\rho N_{av} \times [x(Z_A + \Delta f'_A) + y(Z_B + \Delta f'_B)]}{M} \quad (5)$$

where *M* is the molecular weight. The depth of x-ray penetration varies sigmoidally as a function of α, with a rapid increase at the critical angle of incidence (Fig. 1b). By varying the angle of incidence, it was possible to profile phase transformations as a function of irradiated depth of penetration, τ, and this is referred to as the tau (τ) profile.

Two types of transformations were evaluated using this technique: (i) crystallization of partially amorphous indomethacin and (ii) anhydrate → monohydrate conversion in theophylline. Milling, one of the commonly used pharmaceutical processing steps, caused amorphization of indomethacin (19). This was expected to cause a pronounced increase in the solubility and dissolution rate of indomethacin. However, amorphous indomethacin crystallized in aqueous medium due to which the calculated solubility and dissolution rates were not actualized (10). Considering that indomethacin is practically insoluble in water, such phase transformations *in vivo* can have therapeutic implications.

In case of theophylline, the monohydrate is the stable phase in contact with water at temperatures <66°C (20). During aqueous dissolution studies of anhydrous theophylline, biphasic profiles were obtained and were attributed to the theophylline anhydrate → theophylline monohydrate transformation *during* the dissolution run. The observed dissolution rates will be dictated by the kinetics of anhydrate → monohydrate transformation, which will be governed by the physical form of the anhydrate. Because the physical form of the anhydrate can be influenced by pharmaceutical processing, the dissolution behavior of the granulated anhydrate was also evaluated.

There were three objectives in this project. (i) To systematically study the effect of processing-induced phase

Indomethacin		Pronounced decrease	Aqueous wet	Crystallinity
	Milling	in crystallinity	granulation and drying	substantially regained
(Case I)	⟶	(Case II)	⟶	(Case III)

Scheme 1. Processing induced alterations in the crystallinity of indomethacin.

transformations on drug dissolution rate. Specifically, the influence of processing-induced loss in indomethacin crystallinity and anhydrate → hydrate→ anhydrate phase transformations during processing of theophylline was evaluated. (ii) To develop glancing angle XRD as a technique to profile phase transformations *during* dissolution as a function of tablet depth. (iii) To apply this technique to study phase transformations *during* the dissolution of indomethacin and theophylline tablets. Numerous studies have dealt with the effect of pharmaceutical processing on the solid state of the drug (21). However, the influence of phase transformations during dissolution on product performance has not been adequately evaluated.

MATERIALS AND METHODS

Materials

Indomethacin (γ-polymorph) and anhydrous theophylline, obtained from Sigma Chemical Co. (St. Louis, MO, USA), were used as received. The drugs were subjected to various processing steps (Schemes 1 and 2).

Scheme 1

Substantially crystalline indomethacin (case I) was milled for 15 min (referred to as case II). Milled indomethacin was wet-granulated and dried (case III).

Scheme 2

Anhydrous theophylline (referred to as case I) was wet-granulated and the resulting granules (case II) were stored in a chamber at 75% relative humidity (RH) until a water content of ~9% w/w was achieved (stoichiometric water content of theophylline monohydrate). The granules were then dried at 50°C in an oven under ambient pressure, and the resulting phase was referred to as case III.

The phase transformations of both indomethacin and theophylline were monitored by conventional x-ray diffractometry (XRD), differential scanning calorimetry (DSC), thermogravimetric analysis (TGA), and Karl Fischer titrimetry (KFT).

Methods

Conventional XRD

About 200 mg of sample was exposed to Cu Kα radiation (45 kV × 40 mA) in a wide-angle powder x-ray diffractometer (model D5005, Siemens, Madison, WI, USA). The instrument was operated in the step-scan mode, in increments of 0.05°2θ. The angular range was 5 to 40°2θ and the counts were accumulated for 1 s at each step. The data collection and analyses were performed with commercially available software (Jade, version 5.0, Materials Data Inc., Livermore, CA, USA).

Determination of Crystallinity

The crystallinity determinations were performed by XRD wherein the unprocessed drug (i.e., "as is") was considered to be 100% crystalline. The peak height (peaks at 12.3°2θ and 12.6°2θ for indomethacin and theophylline, respectively) of the processed samples was compared to that of the "as-is" drug. An increase in lattice disorder resulted in a decrease in peak height.

Thermal Analysis

A differential scanning calorimeter (model 910, TA Instruments) and a thermogravimetric analyzer (model 951, TA Instruments, New Castle, DE, USA) were connected to a thermal analysis operating system (Thermal Analyst 2000, TA Instruments). About 4 mg of the sample was weighed into an aluminum pan, which was crimped nonhermetically and heated in the differential scanning calorimeter from room temperature to ~300°C. In the thermogravimetric analyzer, the samples were heated in an open aluminum pan from room temperature to ~300°C. In both cases, the samples were heated at 10°C/min, under nitrogen purge.

Karl Fischer Titrimetry

The water content was determined using a Karl Fischer titrimeter (model CA-05 Moisture Meter, Mitsubishi, Tokyo, Japan).

Scanning Electron Microscopy

Either 200 mg (indomethacin) or 300 mg (theophylline) of the sample was placed in a circular stainless steel holder and compressed in a hydraulic press (Carver Model C Laboratory press, Menomonee Falls, WI, USA) to either ~130 MPa (indomethacin) or 140 MPa (theophylline) for 1 min. The diameter of the compact was 1 cm. The samples were mounted on SEM stubs with double-sided carbon tape and coated with platinum (50 Å) and observed under a scanning electron microscope (Hitachi S-800). To evaluate phase transformations during dissolution, indomethacin and theophylline compacts were immersed in the dissolution medium for ~2 h and 30 s, respectively, and subjected to SEM. Selected theophylline samples were subjected to XRD after the SEM

Anhydrate	Aqueous wet granulation	Hydrate	Drying at 50°C under ambient pressure	Anhydrate
(As is, case I)	⟶	(Case II)	⟶	(Case III)

Scheme 2. The different phases obtained on processing anhydrous theophylline.

studies. This was done to confirm that there were no phase transformations during sample preparation and analysis.

Intrinsic Dissolution Rate The intrinsic dissolution rates (IDRs) were obtained in a modified Wood's apparatus using phosphate buffer (pH 7.2) as the dissolution medium (22,23). The samples were placed in a stainless steel holder and compressed in a hydraulic press (Carver Model C Laboratory press) to ~130 MPa (indomethacin) or 140 MPa (theophylline) for 1 min. The sample holder with the compacted powder was screwed into the base of a poly methylmethacrylate cylinder such that only a single face of the compact (area, 0.79 cm^2) was exposed to the medium. The cylinder was then placed in a water bath (24°C ± 0.5°C). The dissolution medium was stirred with a three-bladed paddle (Slo Syn, Superior Electric Co., Rockford, IL, USA) placed directly above the compact. Samples were withdrawn at predetermined intervals, filtered, and the concentration of drug in solution monitored by UV spectrophotometry (Beckmann DU 7400, Fullerton, CA, USA). The experimental and sampling time interval details are as follows.

Indomethacin. The dissolution medium (750 ml of pH 7.2 phosphate buffer), specified by the USP, was stirred at 75 rpm. The dissolution studies were carried out for 2 h, and samples were withdrawn at 2.5, 5, and 10 min and every 10 min thereafter. The concentration of drug in solution was determined by UV spectrophotometry at 318 nm.

Theophylline. The dissolution medium (900 ml of distilled water), specified by the USP, was stirred at 50 rpm. The dissolution experiments were carried out for 5 min, and samples were withdrawn every 30 s, filtered, and the concentration of the drug in solution monitored by UV spectrophotometry at 272 nm (Beckmann DU 7400).

In case of both drugs, the dissolution experiments were carried out under sink conditions; that is, the maximum concentration of the drug in the medium during the experiments was less than 15% of its saturation solubility.

Glancing Angle XRD

Instrumentation. The samples were exposed to nickel-filtered Cu Kα radiation (45 kV × 40 mA) in a wide-angle powder x-ray diffractometer (model Dmax B, Rigaku, Tokyo, Japan) with a 0.1° incidence slit and a 0.15° receiving slit. The instrument was operated in a step-scan mode in increments of 0.05°2θ, and counts were accumulated for 1 s at each step. The measurements were carried out at incident angles ranging from 0.1 to 5°.

Alignment. A 0.05° incidence slit, two absorbers, and a 0.15° receiving slit were used to align the instrument. The operating power was 10 kV × 5 mA, the tube height was adjusted for maximum intensity, and the 2θ angle was calibrated. A beam split plate was placed in the sample chamber, and the height of the stage was adjusted so that only half the intensity of the x-ray beam reached the detector. This alignment was checked before every analysis.

The instrument alignment and sensitivity were checked using Standard Reference Materials (SRMs) obtained from the National Institute of Standards and Technology (NIST). Silicon powder (SRM 640c) is certified for use as a standard for calibration of peak positions in powder diffractometry. Zinc oxide and titanium dioxide (SRM 674a) are certified for use as internal standards for quantitative XRD and as external standards to determine the intensity response of diffractometers. The critical angles of incidence (α_c) of these standards were determined experimentally and compared with the values calculated using Eq. (2). The integrated intensities of the characteristic peaks of the three standards were determined and then plotted against α (ranging from 0.1° to 5°), and α_c was the point of maximum slope. The difference between the experimentally determined and the calculated values were <11% (Table I).

Sample Preparation. The samples were compacted in a hydraulic press at ~130 MPa (indomethacin) or 140 MPa (theophylline) for 1 min. The flat-faced compacts were about 1 cm in diameter and 1 mm (indomethacin) or 2 mm (theophylline) thick. An aluminum x-ray sample holder with a circular cavity was fabricated. A small piece of molding clay was put at the bottom of this cavity, the compact placed into the cavity, and then using a glass slide it was gently pressed down until the holder and the compact surfaces were coplanar.

Method of Analysis

Indomethacin. The integrated intensities (II_i) of the 12.3°2θ peak of the dry compacts were obtained at α values ranging from 0.1° to 5°. About 0.5 ml of the dissolution medium was placed on the upper surface of the compact and left undisturbed for 2 h. Excess liquid was wiped off and the integrated intensities of the same peak was monitored again (II_f). The fractional increase in indomethacin crystallinity was expressed as:

$$\frac{II_f - II_i}{II_f} \tag{6}$$

Equation (1) enabled us to calculate the depth of x-ray penetration as a function of the incident angle. By combining Eqs. (1) and (6), the fractional increase in crystallinity was then plotted as a function of the distance from the compact surface (depth of penetration).

Theophylline. In this case, the characteristic peak of anhydrous theophylline at 12.6°2θ was monitored. The procedure outlined earlier was used except that the compacts were exposed to aqueous medium for either 30 or 300 s. The fraction of theophylline anhydrate converted at each angle of incidence (α) was expressed as:

$$\frac{II_i - II_f}{II_i} \tag{7}$$

Table I. The Critical Angle of Incidence of Three Standard Reference Materials Determined Experimentally and Using Eq. (2)

Sample	Experimentally determined critical angle (degrees)	Calculated value of critical angle (degrees)	Percentage deviation from calculated value
Silicon	0.20	0.22	–9.0
Zinc oxide	0.29	0.32	–10.7
Titanium dioxide	0.30	0.29	1.7

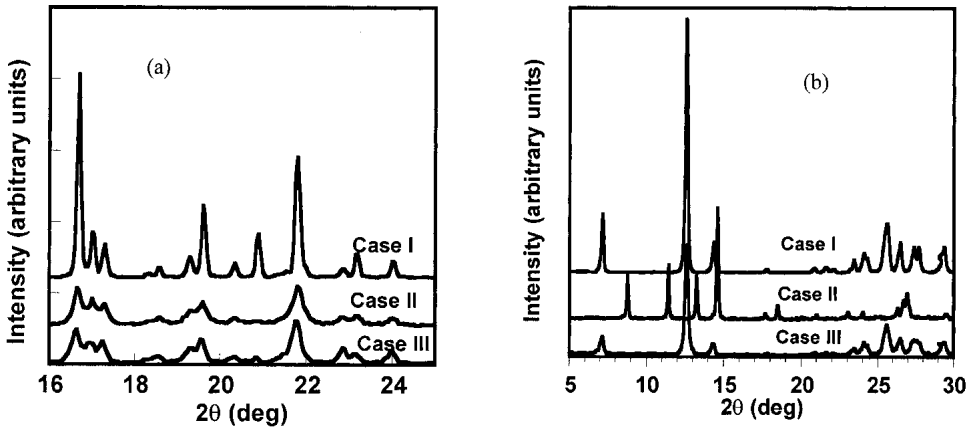

Fig. 2. Powder x-ray diffraction (XRD) patterns of (a) indomethacin and (b) theophylline after different processing steps. Schemes 1 and 2 describe the processing steps.

RESULTS AND DISCUSSION

Indomethacin

The XRD pattern of the unprocessed drug (Scheme 1, case I) matched that of the anhydrous γ-polymorph (Fig. 2a) (24). In the DSC, only a single endotherm attributable to melting was observed at ~161°C, in good agreement with the reported melting temperature (25). XRD studies revealed that milling for 15 min caused an ~45% decrease in crystallinity (case II; Fig. 2a). The formation of amorphous indomethacin was also evident from the observed glass transition at ~40°C, which agreed well with the reported value of 42°C (26). When the milled sample was wet-granulated and dried (Scheme 1, case III), the crystallinity was partially regained (crystallinity of case III was ~33% lower than that of the "as is"). The processing steps affected only the degree of crystallinity with no effect on the polymorphic form (Fig. 2a). Because the dissolution rate is inversely related to the degree of crystallinity, the expected order of dissolution rate was case II > case III > case I.

The intrinsic dissolution profiles (Fig. 3a) were nonlinear, and this could be attributed to (i) a phase transformation during the dissolution experiment and/or (ii) dissolution under nonsink conditions. While the aqueous solubility (at pH 7.2) of indomethacin is ~0.08 mg/ml at 25°C (27), the highest drug concentration in solution was ~0.006 mg/ml, which is less than 8% of the saturation solubility. Hence, it is reasonable to assume that sink conditions were maintained throughout the experiment. Therefore, the observed nonlinearity was probably due to phase transformations during dissolution. Compacts of milled indomethacin (case II) were analyzed both by SEM and glancing angle XRD before and after exposure to the dissolution medium.

While SEM revealed extensive crystallization on exposure to the dissolution medium (data not shown), glancing angle XRD enabled depth profiling of this process (Fig. 4 a and b). While the depth of penetration as a function of incident angle was calculated using Eq. (1), the phase composition was determined using Eq. (6). This then enabled us to plot the increase in indomethacin crystallinity as a function of depth of penetration. The fitted curve, an exponential function, is referred to as the tau (τ) profile (28). The τ profiles of several indomethacin compacts were obtained, and two representative profiles are presented in Fig. 4 a and b. In case of the milled drug (case II), there was substantial crystallization at the surface. The fraction crystallized decreased as a function of compact depth. The profile shapes of the two com-

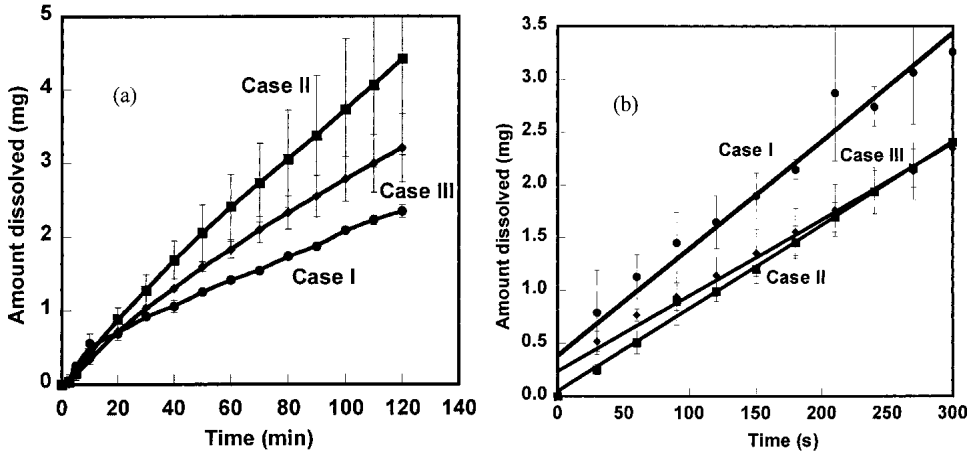

Fig. 3. The intrinsic dissolution profiles of (a) indomethacin and (b) theophylline at different processing steps. Cases I (●), II (■), and III (♦) are described in Schemes 1 and 2. Error bars represent standard deviations (n = 3).

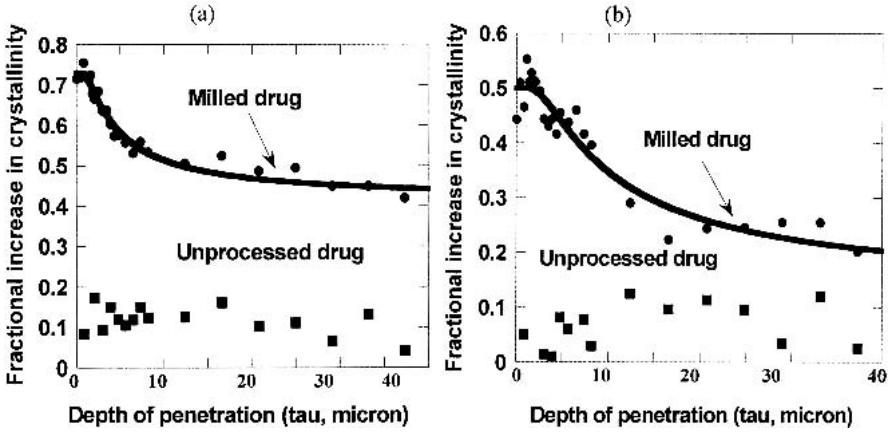

Fig. 4. Fractional increase in the crystallinity of indomethacin as a function of the distance from the compact surface. The compacts prepared with milled indomethacin had been exposed to the dissolution medium for 2 h. The filled circles are the experimental data points; the tau profile is an exponential function fitted to this data. For the sake of comparison, the results obtained with the unprocessed drug (case I) have also been presented (filled squares). Because a phase transition was not expected in this case, no attempt was made to fit the data. The results of two individual compacts (a and b) are presented.

pacts, reflecting the fractional change in crystallinity as a function of tablet depth, were very similar. Because dissolution occurs from the tablet surface, this region is of predominant interest to us. On exposure to the medium for 2 h, while there was ~75% increase in crystallinity at the surface of one compact (Fig. 4a), there was only a 55% increase in the other (Fig. 4b). This variability can be attributed to several factors including preferred orientation of the drug powder during compression and the compact microstructure. These differences in crystallization kinetics may be responsible for the observed variability in the dissolution profile of the milled drug (case II; Fig. 3a). There appeared to be a gradual decrease in dissolution rate and this was attributed to drug crystallization during the experiment. Thus, the glancing angle XRD results explain the observed dissolution profiles. As is evident from Fig. 4 a and b, this change in crystallinity was highest in case II.

Because the profiles of cases I, II, and III were nonlinear, dissolution rates could not be calculated (Fig. 3a). Therefore, the amount of drug dissolved at the individual time points were compared by the one-way ANOVA test ($\alpha = 0.05$). As expected, the amount dissolved at any time t could be rank-ordered as case II > case III > case I. However, the amount dissolved in the processed samples (cases II and III) were not significantly different whereas the unprocessed drug (case I) exhibited a significant difference (observed order: case II ≈ case III > case I). Due to crystallization during the dissolution experiment, the difference in the degree of crystallinity of processed samples (cases II and III) did not translate to a significant difference in dissolution behavior.

The experimentally observed dissolution behavior of metastable phases will be governed by (i) dissolution rate of the metastable form, (ii) rate of crystallization of the stable form, and (iii) dissolution rate of the stable form. When the dissolution rate > metastable to stable transformation rate, the observed dissolution behavior is expected to be that of the metastable phase or a mixture of the metastable and stable phases. This was the case in indomethacin, wherein the kinetics of drug crystallization was slow. As a result, the processing-induced decrease in crystallinity translated to accelerated drug dissolution. However, there are instances where the transformation rate ⩾ dissolution rate, as was observed in theophylline (discussed later).

It was evident from the glancing angle studies that the extent of metastable → stable transformation was maximum at the compact surface (Fig. 4). This is attributed to the intimate contact of the compact surface with the dissolution medium. Because drug dissolution occurs from the compact surface, the dissolution behavior will be dictated by the surface phase composition. Glancing angle XRD enabled us to not only determine the surface phase composition, but also the profile phase transformations as a function of compact depth.

Theophylline

The x-ray diffraction pattern of the unprocessed drug (case I in Scheme 2) indicates that it was the stable anhydrate and was substantially crystalline (Fig. 2b). This pattern matched that in the Powder Diffraction Files (PDF) of the International Centre for Diffraction Data (ICDD) (29). The endotherm observed at ~272°C in the differential scanning calorimetric curve (not shown) was in good agreement with the reported melting temperature range (270–275°C) in *The Merck Index* (30). Granulation (of case I) with water resulted in the formation of theophylline monohydrate (case II in Scheme 2; Fig. 2b). The peak positions were consistent with the reported powder pattern of theophylline monohydrate (31). Two endotherms were observed in the DSC curves; the broad endotherm over the temperature range 60–100°C attributable to dehydration and water vaporization, followed by melting of the anhydrate at ~272°C. Drying (of case II) resulted in complete dehydration and yielded the anhydrate (case III in Scheme 2; Fig. 2b). While case III was the same polymorph as case I, its crystallinity was ~25% lower.

This decreased crystallinity was expected to result in a higher dissolution rate than that of case I. The dissolution rate was expected to be the lowest in case II (hydrate). The intrinsic dissolution profiles were linear, and the order of dissolution rates was case I > case II ≈ case III (Fig. 3b). At 25°C,

the aqueous solubility of anhydrous theophylline is ~13.6 mg/ml and that of theophylline monohydrate is ~8 mg/ml (20). Therefore, based on the crystallinity and state of hydration of these three cases, the expected order was case III > case I > case II. Interestingly, the dissolution rate of case III (anhydrate of reduced crystallinity) was not significantly different (ANOVA; $\alpha = 0.05$) from that of case II, which was the monohydrate.

From Fig. 5a, it is apparent that on exposure to aqueous medium, theophylline anhydrate transformed to theophylline monohydrate (appearance of peaks unique to theophylline monohydrate). However, the intensity of the hydrate peaks was higher in case III compacts (Fig. 5b) than in case I, which indicated that the amount of hydrate formed was more in case III. This could be due to the fact that the amorphous regions in case III dissolved at a faster rate, achieving supersaturation more rapidly and hence having a higher rate of hydrate crystallization. Due to this rapid conversion, dissolution profile of case III was similar to that of the hydrate (Fig. 3b). Because the unprocessed drug (case I; Fig. 3b) did not convert as readily to the hydrate, the observed profile substantially reflected the dissolution rate of the anhydrate. Scanning electron microscopy provided direct visual evidence of crystallization (Fig. 5; insets).

Next, glancing angle XRD was used to profile these transformations as a function of tablet depth. Anhydrous theophylline tablets were immersed in water for either 30 or 300 s. While the depth of penetration as a function of incident angle was calculated from Eq. (1), the phase composition was determined using Eq. (7). This then enabled us to plot the volume fraction of the anhydrate converted as a function of depth of penetration. At the surface of tablets prepared from the unprocessed anhydrate (case I), there was ~78% conversion to theophylline monohydrate whereas ~92% conversion had occurred in case III tablets (Fig. 6a). Processing caused a decrease in anhydrate crystallinity (Fig. 2b), accelerating the monohydrate formation when placed in contact with the dissolution medium. Consequently, the dissolution rate of case III was < case I. As expected, when the exposure time was increased to 300 s, the extent of conversion was higher in both case I and III tablets (Fig. 6b). Thus, the pharmaceutical processing steps of wet granulation followed by drying resulted in a decrease in the crystallinity of the anhydrate (i.e., activation of the solid). Although processing induced only a modest decrease in crystallinity, the effect on dissolution rate was quite pronounced.

Method Validation

The XRD of organic materials poses some unique challenges. Typically, their unit cells are large with low symmetry, leading to peaks in the low angular range. From the standpoint of accuracy, this is undesirable. Second, the low mass attenuation coefficients lead to high specimen transparency. Finally, problems due to preferred orientation are frequently encountered (32). We were cognizant of these potential problems during the method development. The instrument alignment was checked before each analysis. In an effort to improve the accuracy in the lower angular range, a very small (0.1°) incident slit was used. For every sample, because the quantification of phase transformation during dissolution was based on the change in intensity with respect to the dry compact, the errors due to preferred orientation were expected to be small.

There were some additional issues specifically associated with our experimental procedure: (i) because phase transformations during dissolution were being analyzed, a potential problem was the change in depth of x-ray penetration due to the phase change; (ii) possible signal attenuation due to the presence of water; and (iii) phase changes occurring during experimental timescales.

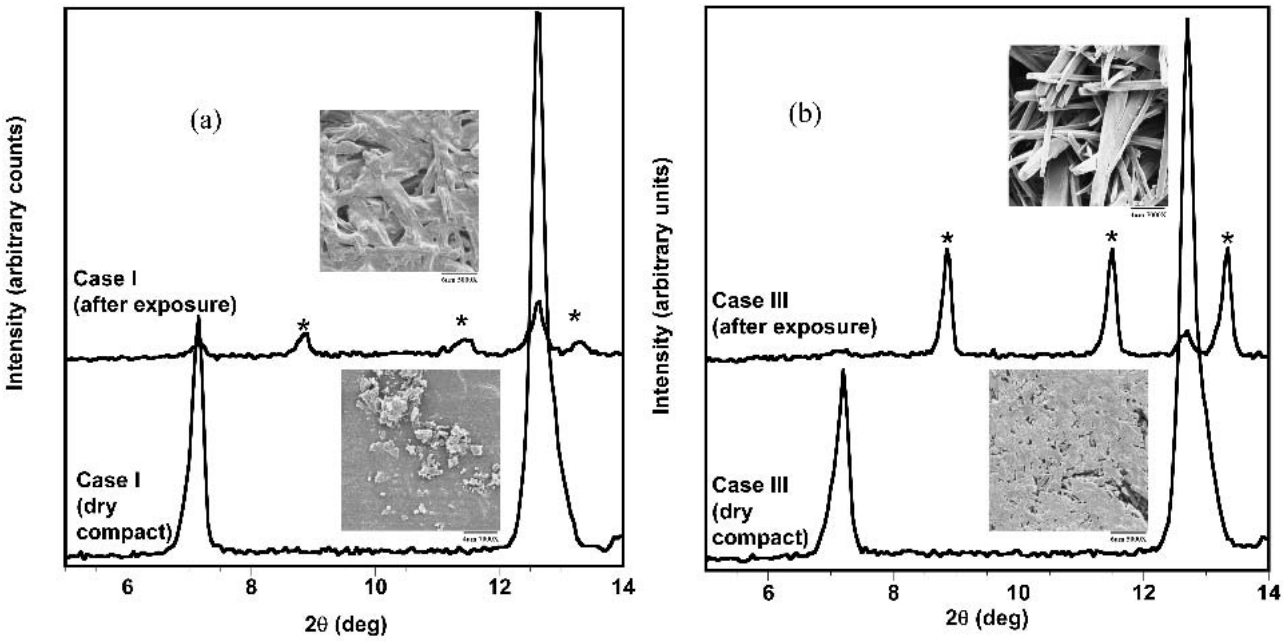

Fig. 5. XRD patterns of (a) case I ("as-is" anhydrate) and (b) case III (anhydrate formed by dehydration of theophylline monohydrate) tablets before (lower curve) and after (upper curve) exposure to dissolution medium for 5 min. Peaks marked with an asterisk are unique to theophylline monohydrate. The insets contain the corresponding SEM photomicrographs.

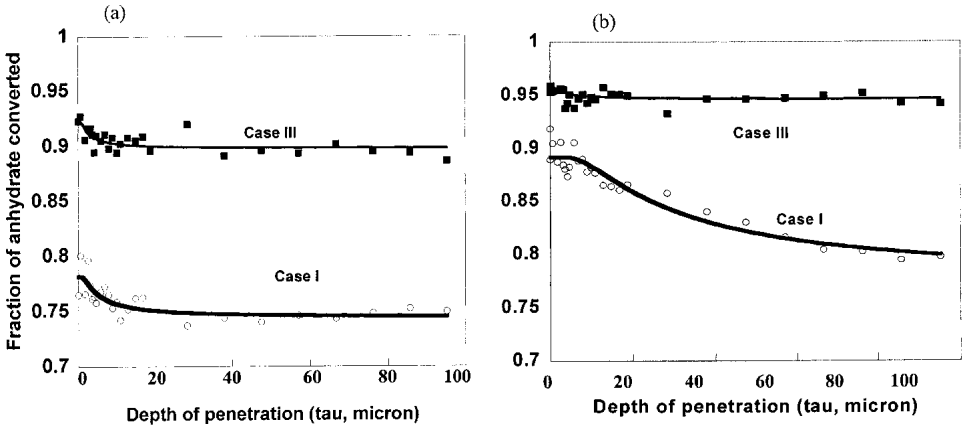

Fig. 6. Fraction of anhydrous theophylline converted to theophylline monohydrate as a function of tablet depth following exposure to the dissolution medium for (a) 30 s and (b) 300 s. The open circles (◯) are the experimental data points for unprocessed anhydrous theophylline (case I). The filled squares (■) are the experimental data points for the anhydrate formed by dehydration of the monohydrate (case III). The tau profile (solid curve) has been fitted to the experimental data points.

Effect of Phase Transformation on Depth of Penetration

We used glancing angle XRD to monitor the increase in indomethacin crystallinity and theophylline anhydrate → theophylline monohydrate transition. These transitions will change the density and therefore the microstructure of the compact. In case of theophylline, a change in molecular weight will also alter the mass attenuation coefficient. We therefore calculated the effect of these phase transformations on the depth of penetration of x-rays (Table II). It is evident that the phase transformation had a small effect on the depth of penetration.

Signal Attenuation by Sorbed Water

Because the tablets sorbed water when exposed to the dissolution medium, it was necessary to determine whether this residual liquid attenuated the diffracted signal. The mass attenuation coefficient of indomethacin and theophylline are listed in Table II; that of water is 10.3 cm^2/g. The low mass attenuation coefficient of water is not expected to cause significant signal attenuation. However, this was confirmed by the following experiments.

A compact of the substantially crystalline indomethacin sample was exposed to the dissolution medium for 30 min and the integrated intensity of the peak at ~12.3°2θ was determined before and after exposure to the dissolution medium (α ranging from 0.1° to 5°). There was only a 4.4% w/w (±1.4%) water uptake and no significant signal attenuation could be observed (Fig. 7a). Ideally, this study should have been carried out in partially crystalline indomethacin. However, because water sorption results in crystallization, we were forced to use the crystalline drug.

Because theophylline monohydrate does not undergo any phase transformation when placed in contact with water, it was used to evaluate signal attenuation by sorbed water. The stoichiometric water content in the monohydrate is 9% w/w. A sample containing ~25% w/w water (determined by TGA) was compressed to form a compact. The integrated intensity of the peak at ~11.6°2θ (unique to theophylline monohydrate) was determined at α values ranging from 0.1° to 0.5°. The compact was then air-dried to a water content of ~9% w/w, when only the lattice water was retained (confirmed by conventional XRD). The integrated intensity of the 11.6°2θ peak was monitored. The difference between the two could be attributed to sorbed water. At $\alpha > 0.2°$, the difference was consistently ≤7% whereas it was negligible at $\alpha \geq 0.5°$ (Fig. 7b). Because most of the depth profiling was based on $\alpha > 0.2°$, the effect of the sorbed water is minimal, if any.

Table II. Depth of Penetration of X-Rays in Indomethacin and Theophylline Compacts and Other Relevant Properties of Indomethacin and Theophylline

Sample	Density (g/cm^3)	Mass attenuation coefficient (cm^2/g)[a]	Molecular weight (g/mol)	Depth of penetration (μm)[b]
Indomethacin				
Before exposure to dissolution medium	1.3[c]	15.4	238.2	~42
On exposure to dissolution medium	1.3[c]	15.4	238.2	~43
Theophylline				
Anhydrous theophylline	1.4[d]	6.5	180.2	~95
Theophylline monohydrate	1.4[d]	6.5	198.2	~91

[a] Cu Kα radiation.
[b] Calculated using Eq. (1) at an angle of incidence of 5°.
[c] Determined by helium pycnometry [in good agreement with the literature (26)].
[d] From the Powder Diffraction Files of the International Centre for Diffraction Data (ICDD) database.

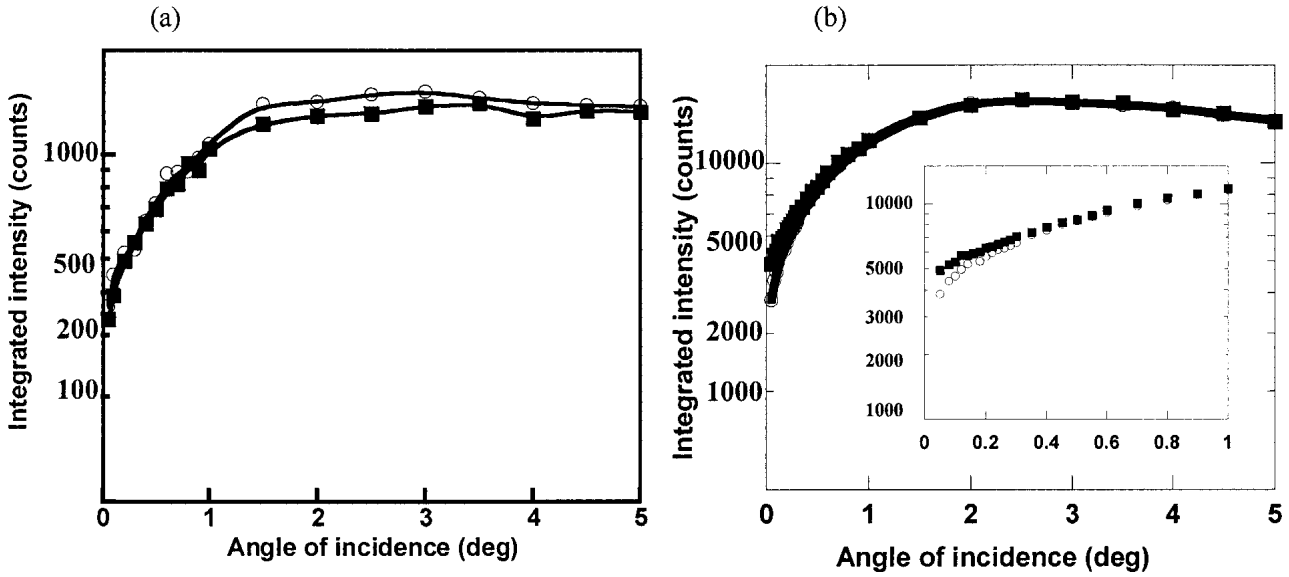

Fig. 7. Effect of water content on the integrated intensity of (a) the 12.3°2θ peak of indomethacin as a function of the angle of incidence (○) before and (■) after exposure to the dissolution medium and (b) the 11.6°2θ peak of theophylline monohydrate, (○) 25% w/w water, (■) 9% w/w water. Inset: the intensity values at lower incident angles (0.1° to 1°).

Phase Changes Occurring During Experimental Timescales

During evaluation of anhydrate → hydrate transformation in theophylline, the tablets were exposed to the dissolution medium either for 30 or for 300 s. However, due to the presence of sorbed water, further anhydrate → hydrate transformation may occur *during* the timescale of the glancing angle XRD experiment. In order to determine the extent of this transition, two experiments were performed.

An anhydrous theophylline compact was exposed to the dissolution medium for either 30 or 300 s. The excess water was wiped off, and the intensity of the peak at 12.6°2θ was obtained by setting $\alpha = 5°$. The angular range of the scan was 10.6 to 12.3°2θ, requiring ~35 s for each scan. The experiment was repeated for ~25 min. In the sample exposed to the medium for 30 s, there was a sharp decrease in the peak intensity for the first 5 min (Fig. 8a) revealing phase transformation *during* the x-ray analysis. Thereafter, the peak intensity was essentially constant. Therefore, the glancing angle experimental data obtained during the first 5 min were deemed unreliable and were discarded. Based on these results, we conclude that we have overestimated the extent of conversion in the sample exposed to the dissolution medium for 30 s (Fig. 6a). When the above experiment was repeated after exposing the theophylline compact to the dissolution medium for 5 min, there was no change in the integrated intensity (data not shown). Therefore, in this case, there are no changes in the sample during the timescale of the glancing angle XRD work (Fig. 6b).

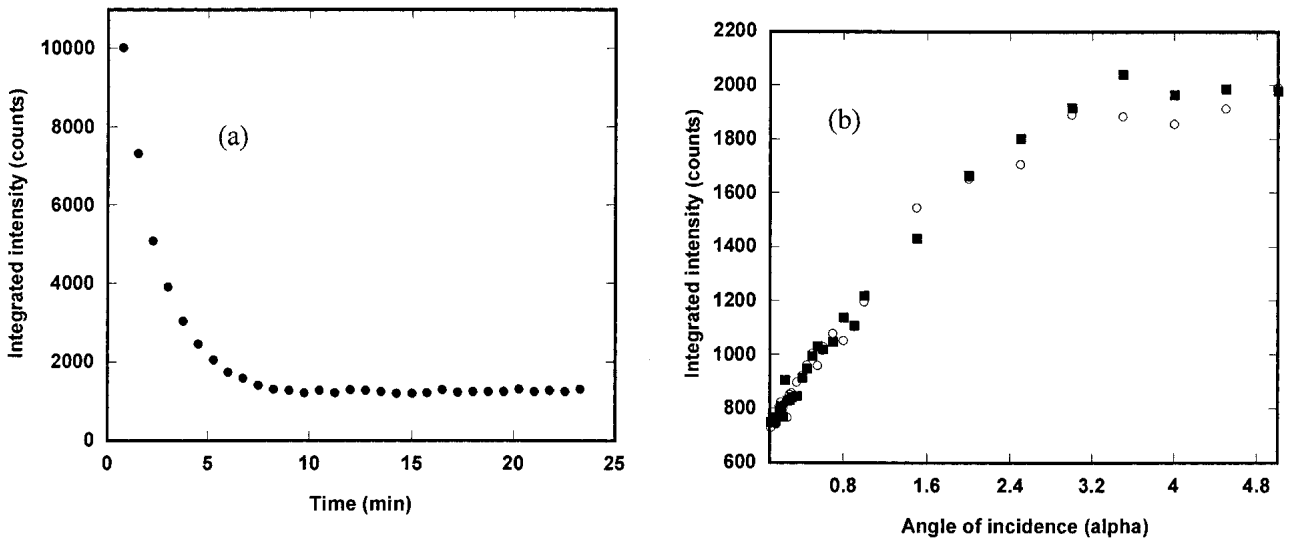

Fig. 8. (a) Integrated intensity of the 12.6°2θ peak of theophylline anhydrate at a 5° angle of incidence after exposure to the dissolution medium for 30 s. (b) Integrated intensity of the 12.6°2θ peak of theophylline anhydrate at incident angles ranging from 0.1° to 5°. The compact was exposed to the dissolution medium for 30 s. The open circles (○) are the data from the first scan and the filled squares (■) were obtained from the second scan.

While we recognize that there is an overestimation of the anhydrate → hydrate transformation in the samples exposed to the dissolution medium for 30 s (Fig. 6a), the difference between the processed (case III) and unprocessed (case I) drug is real. The high reactivity of processed theophylline (case III) is evident from the nearly identical profiles obtained following exposure to the dissolution medium for either 30 or 300 s (Fig. 6 a and b). In light of this high reactivity, the actual difference between cases I and III would be more pronounced than that measured experimentally (Fig. 6a).

In the second experiment, the compacts were exposed to the medium for 30 s and the integrated intensity of the peak at 12.6°2θ was monitored at incident angles ranging from 0.1 to 5°, requiring ~40 min for completion. The analysis was then repeated over the same angular range. The object was to monitor any phase transformation *during* the experiment. Discarding the data obtained during the first 5 min (justification provided earlier), there was no systematic change in the diffracted intensities between the first and second runs (Fig. 8b). We carried out the same experiment, after exposing the compact to the dissolution medium for 5 min. At all time points (including the first 5 min), the intensities from the two analyses were very similar (data not shown).

Significance

Most analytical techniques, including conventional wide-angle XRD, enable "bulk" or "averaged" analysis of a powder bed. Conventional XRD patterns are obtained over the angular range of 2–40°2θ. The depth of penetration of x-ray will be dependent on the incident angle of the x-rays. For example, at an incident angle of 15°2θ, the depth of penetration in an organic pharmaceutical (characterized by a low mass attenuation coefficient), will be ~1 mm. However, in glancing angle XRD, the depth of x-ray penetration, again depending on the incident angle, can be of the order nanometers and micrometers. This technique permitted us to quantify and thereby profile phase transformations as a function of compact depth. This technique has potential utility in monitoring surface reactions—both chemical decomposition and physical transformations. By combining glancing angle with conventional XRD, it is possible to determine the effect of storage on the phase composition at the tablet surface and bulk. For example, it is possible to depth-profile hydration (or dehydration) reactions, crystallization, and polymorphic transformations. Similarly, chemical reactions can be investigated, provided the reactant and/or the product are crystalline. In coated tablets, there is potential to characterize not only the coating and core simultaneously, but also any interactions between the two.

Limitations

The low mass attenuation coefficient and potential preferred orientation are the major sources of error when dealing with organic pharmaceuticals. In contrast to metals and semiconductors, which are relatively "inert," phase transformations in pharmaceuticals can be significantly influenced by numerous factors including temperature, water vapor pressure, and the tablet microstructure. This could explain the high variability in the observed transformations kinetics.

CONCLUSIONS

Milling of indomethacin resulted in a decrease in crystallinity, which was partially regained during the subsequent aqueous wet granulation process. Crystallization of the drug occurred *during* the intrinsic dissolution run. The dissolution rate of partially crystalline indomethacin was higher than that of the "as-is" crystalline drug. This was attributed to the low crystallization rate of the amorphous indomethacin in contact with the dissolution medium.

When highly crystalline anhydrous theophylline was granulated with water, it transformed to theophylline monohydrate. During drying, the hydrate transformed back to the anhydrate, but with a lower crystallinity. Theophylline anhydrate → monohydrate transformation occurred during intrinsic dissolution studies, and the conversion rate depended on the crystallinity of the drug. The transformation rate was higher when drug crystallinity was lower.

In both these systems, several processes occurred simultaneously: (i) dissolution of the metastable form, (ii) crystallization of the stable form, and (iii) dissolution of the stable form. The observed dissolution rate is dictated by the kinetics of these processes. When the dissolution rate ≪ metastable to stable transformation rate, the dissolution rate of the transformed (i.e., stable) phase is obtained. This was observed in the theophylline system, wherein the poorly crystalline anhydrate rapidly converted to the monohydrate (Fig. 2b, case III; Fig. 6 a and b, case III). Otherwise, the observed dissolution rate is expected to be that of a mixture of the metastable and stable phases as in the case of indomethacin.

It is instructive to recognize that when dealing with compacts as well as powder particles, dissolution occurs from the surface. Because the surface is in intimate contact with the medium, the extent of phase transformation is expected to be maximum at the compact surface. This necessitates profiling phase composition as a function of compact depth so as to understand the observed dissolution behavior. We have established the utility of glancing angle XRD for such a purpose.

In drugs exhibiting dissolution rate limited absorption, there is a potential to enhance bioavailability by using the metastable forms. However, the use of metastable phases is seriously limited by their physical instability, both during manufacture and storage. We have demonstrated that it is also necessary to ensure their stability *during* dissolution. The solubility advantage can be negated if there is transformation during dissolution.

REFERENCES

1. L. Lachman, H. A. Lieberman, and J. L. Kanig. *The Theory and Practice of Industrial Pharmacy*. Lea & Febiger, Philadelphia, 1986.
2. A. J. Aguiar, K. C. J. John, A. W. Kinkel, and J. C. Samyn. Effect of polymorphism on the absorption of chloramphenicol from chloramphenicol palmitate. *J. Pharm. Sci.* **56**:847–853 (1967).
3. K. Kimura, F. Hirayama, and K. Uekama. Characterization of tolbutamide polymorphs (Burger's forms II and IV) and polymorphic transition behavior. *J. Pharm. Sci.* **88**:385–391 (1999).
4. Y. Kobayashi, S. Ito, S. Itai, and K. Yamamoto. Physicochemical properties and bioavailability of carbamazepine polymorphs and dihydrate. *Int. J. Pharm.* **193**:137–146 (2000).
5. Federal Register Part V and F. Department of Health and Human Services. International Conference on Harmonization; Draft Guidance on Specifications: Test procedures and Acceptance

Criteria for New Drug Substances and New Drug Products: Chemical Substances; Notice, 1997.
6. Y. Chikaraishi, M. Otsuka, and Y. Matsuda. Dissolution phenomenon of the piretanide amorphous form involving phase change. *Chem. Pharm. Bull.* **44**:2111–2115 (1996).
7. A. T. Florence and E. G. Salole. Changes in crystallinity and solubility on comminution of digoxin and observations on spironolactone and estradiol. *J. Pharm. Pharmacol.* **28**:637–642 (1976).
8. Y. Kato and M. Kohketsu. Relationship between polymorphism and bioavailability of amobarbital in the rabbit. *Chem. Pharm. Bull.* **29**:268–272 (1981).
9. M. Ono, Y. Tozuka, T. Oguchi, S. Yamamura, and K. Yamamoto. Effects of dehydration temperature on water vapor adsorption and dissolution behavior of carbamazepine. *Int. J. Pharm.* **239**:1–12 (2002).
10. B. C. Hancock and M. Parks. What is the true solubility advantage for amorphous pharmaceuticals? *Pharm. Res.* **17**:397–404 (2000).
11. H. Vromans, G. K. Bolhuis, C. F. Lerk, and K. D. Kussendrager. Studies on tableting properties of lactose. VIII. The effect of variations in primary particle size, percentage of amorphous lactose and addition of a disintegrant on the disintegration of spray-dried lactose tablets. *Int. J. Pharm.* **39**:201–206 (1987).
12. M. F. Doerner and S. Brennan. Strain distribution in thin aluminum films using x-ray depth profiling. *J. Appl. Phys.* **63**:126–131 (1988).
13. B. L. Ballard, X. Zhu, P. K. Predecki, D. Albin, A. Gabor, J. Tuttle, and R. Noufi. Determination of composition and phase depth-profiles in multilayer and gradient solid solution photovoltaic films using grazing incidence X-ray diffraction. *Adv. X-Ray Anal.* **38**:269–276 (1995).
14. P. Eisenberger and W. C. Marra. X-ray diffraction study of the germanium (001) reconstructed surface. *Phys. Rev. Lett.* **46**:1081–1084 (1981).
15. L. G. Parratt. Surface studies of solids by total reflection of X-rays. *Phys. Rev.* **95**:359–369 (1954).
16. X. Zhu, B. Ballard, and P. Predecki. Determination of z-profiles of diffraction data from tau-profiles using a numerical linear inversion method. *Adv. X-Ray Anal.* **38**:255–262 (1995).
17. T. C. Huang. Surface and ultra-thin film characterization by grazing-incidence asymmetric Bragg diffraction. *Adv. X-Ray Anal.* **33**:91–99 (1990).
18. B. E. Warren. *X-Ray Diffraction*. Addison Wesley, Reading, MA, 1969.
19. M. Otsuka, T. Matsumoto, and N. Kaneniwa. Effect of environmental temperature on polymorphic solid-state transformation of indomethacin during grinding. *Chem. Pharm. Bull.* **34**:1784–1793 (1986).
20. E. Suzuki, K. Shimomira, and K. Sekiguchi. Thermochemical study of theophylline and its hydrate. *Chem. Pharm. Bull.* **37**:493–497 (1989).
21. K. R. Morris, U. J. Griesser, C. J. Eckhardt, and J. G. Stowell. Theoretical approaches to physical transformations of active pharmaceutical ingredients during manufacturing processes. *Adv. Drug Del. Rev.* **48**:91–114 (2001).
22. J. H. Collett, J. A. Rees, and N. A. Dickinson. Some parameters describing the dissolution rate of salicylic acid at controlled pH. *J. Pharm. Pharmacol.* **24**:724–728 (1972).
23. C. Doherty and P. York. Mechanisms of dissolution of frusemide/PVP solid dispersions. *Int. J. Pharm.* **34**:197–205 (1987).
24. M. Otsuka and N. Kaneniwa. A kinetic study of the crystallization process of noncrystalline indomethacin under isothermal conditions. *Chem. Pharm. Bull.* **36**:4026–4032 (1988).
25. M. Yoshioka, B. C. Hancock, and G. Zografi. Crystallization of indomethacin from the amorphous state below and above its glass transition temperature. *J. Pharm. Sci.* **83**:1700–1705 (1994).
26. V. Andronis, M. Yoshioka, and G. Zografi. Effects of sorbed water on the crystallization of indomethacin from the amorphous state. *J. Pharm. Sci.* **86**:346–351 (1997).
27. M. O'Brien, J. McCauley, and E. Cohen. Indomethacin. In K. Florey (ed.), *Analytical Profiles of Drug Substances*, Vol. 13. Academic Press, San Diego, 1984, pp. 211–238.
28. P. Predecki. Determination of depth profiles from X-ray diffraction data. *Powder Diffraction* **8**:122–126 (1993).
29. Powder Diffraction File 26-1893. International Centre for Diffraction Data, Newtown Square, PA, 1997.
30. S. Budaveri, M. J. O'Neil, A. Smith, P. E. Heckelman, and J. F. Kinneary. *The Merck Index*. Merck & Co., Whitehouse Station, NJ, 1996.
31. Powder Diffraction File 27-1977. International Centre for Diffraction Data, Newtown Square, PA, 1997.
32. R. Jenkins. New directions in the X-ray diffraction analysis of organic materials. *Adv. X-Ray Anal.* **35**:653–660 (1991).
33. T. Ely, P. K. Predecki, and I. C. Noyan. A method for obtaining stress-depth profiles by absorption constrained profile fitting of diffraction peaks. *Adv. X-Ray Anal.* **43**:1–10 (2000).